SnO_2-supported palladium catalysts: activity in deNOx at low temperature

D. Amalric-Popescu and F. Bozon-Verduraz *

Laboratoire de Chimie des Matériaux Divisés et Catalyse, Université Paris 7-Denis Diderot, 2, place Jussieu, 75251 Paris Cedex 05, France
E-mail: bonzonver@ccr.jussieu.fr

Received 22 September 1999; accepted 26 November 1999

High surface area tin dioxide (174 m^2/g) has been synthetised and characterised by XRD, TEM and UV-visible DRS. DRS gives evidence for the formation of oxygen vacancies (donor levels) under reducing conditions. CO adsorption gives rise to terminal carbonyl species linked to Sn^{4+} and Sn^{2+}. Palladium–tin oxide catalysts have been prepared from various precursors ($Pd(acac)_2$ and $Pd(NO_3)_2$) and by different preparation methods (grafting, photodeposition); they are active in deNOx reactions at low temperature (180 °C) in the presence of stoichiometric CO–NO–O_2 mixtures. A mechanism involving palladium and oxygen vacancies is proposed.

Keywords: palladium, tin oxides, deNOx, photodeposition, CO adsorption, IR, UV-visible DRS

1. Introduction

Tin dioxide is a n-type semiconductor widely used in sensors [1] and in CO_2 lasers for low-temperature oxidation of carbon monoxide arising from CO_2 dissociation [2]. Despite its reducibility, it has attracted much less attention as a catalyst support than titania (which has been largely used in photocatalysis [3]) or ceria [4] (which has focussed attention in automotive exhaust). Previous works on Pd/SnO_2 catalysts have involved CO oxidation [5a] and selective reduction of NO by hydrocarbons [5b]; some activity in the CO–NO reaction was also found in a preliminary study by Fuller [5c]. The objectives of the present work are (i) to prepare high surface area SnO_2 samples and to characterise their defects by UV-visible DRS; (ii) to obtain well-dispersed SnO_2-supported Pd catalysts by original methods including photodeposition; and (iii) to study their activity in deNOx reactions.

2. Experimental

2.1. Methods

X-ray powder diffraction (XRD) patterns were recorded using a Siemens diffractometer with Co Kα radiation; the crystallite size was estimated using the Scherrer equation. Transmission electron microscopy (TEM) analyses were made on a Jeol 100CXII instrument. FTIR transmission spectra were recorded on a Perkin–Elmer 1730 spectrometer; the samples were pressed into self-supporting discs (about 25 mg/cm^2) and placed in a stainless-steel cell (In Situ Research Instruments) allowing *in situ* analysis of samples in the 20–500 °C range, including CO adsorption. UV-visible-NIR diffuse reflectance spectra (DRS) were recorded on a Cary 5E spectrometer using a Harrick Praying Mantis accessory. The electronic state of Pd was also studied by X-ray photoelectron spectroscopy (XPS).

2.2. Catalyst preparation

SnO_2 was obtained by reaction of nitric acid on high-purity metallic tin; after filtering and washing, the solid was dried at 120 °C and calcined at 200 °C.

Pd/SnO_2: two preparation procedures, original on SnO_2, were used: (i) GC sample: grafting of Pd acetylacetonate on tin dioxide from a solution in toluene at 110 °C for 4 h, filtering, drying of the grafted support at 80 °C for 12 h and calcination under flowing oxygen at 400 °C for 2 h; (ii) PH sample: photodeposition of Pd on the support was carried out by irradiation of a suspension of SnO_2 in a $Pd(NO_3)_2$ solution; the source was a mercury lamp and 2-propanol was used as hole scavenger; after filtration, the solid was dried at 80 °C for 12 h. The Pd content, determined by emission spectroscopy (ICP), was 3.0% for both samples.

3. Results and discussion

3.1. Characterisation of SnO_2

The preparation method leads to rutile-type SnO_2; its characteristics are summarised in table 1. These SnO_2 nanoparticles present a narrow size distribution (figure 1) and a good resistance to sintering (figure 2).

3.1.1. UV-visible DRS

The band gap widths of the SnO_2 sample calcined at 200 °C (3.65 eV) and of a reference SnO (0.7 eV) were

* To whom correspondence should be addressed.

Table 1
Characterisation of tin dioxide.

Particle size (nm)	
(XRD)	4
(TEM)	2–4
Surface area after calcination at 200 °C (m^2/g)	160
Pore volume (cm^3/g)	0.11
Pore diameter (nm)	2.9
Band gap width (eV)	3.6

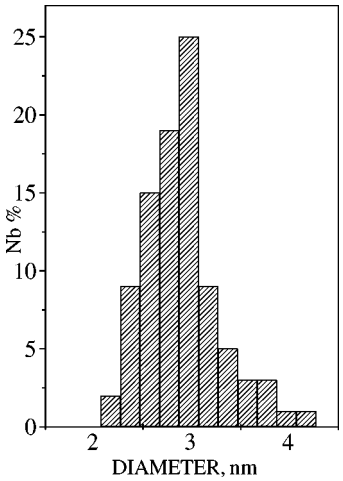

Figure 1. Particle size distribution of SnO_2.

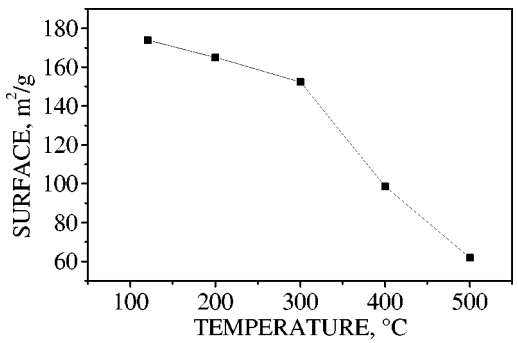

Figure 2. Variation of the surface area with the calcination temperature.

measured from DR spectra (figure 3) according to the Tandon method [6]. In the case of SnO, a quite different value (∼2.3 eV) was reported by Ghiotti [7]. This high value could be ascribed to the presence of intermediate SnO_x phases ($1 < x < 2$), compared to the reference SnO used in this study, which was clearly identified by XRD as the orthorhombic form of tin monoxide (JCPDS no. 24-1342).

After heating SnO_2 *in vacuo* at 400 °C, the spectrum shows a marked absorption in the visible range, adjacent to the interband (valence → conduction) transition (figure 4); this is ascribed to donor levels, such as oxygen vacancies, located within the forbidden band gap. Moreover, CO adsorption generates an additional absorption partially reversible at room temperature.

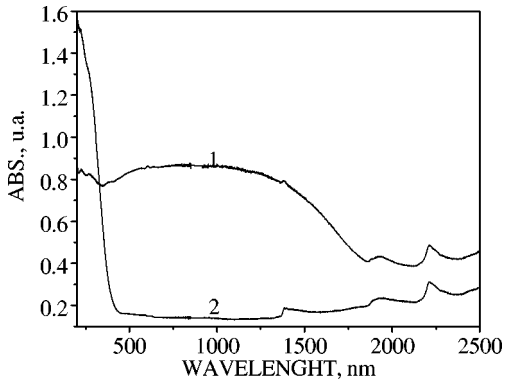

Figure 3. UV-visible DRS in air: (1) SnO (Aldrich) and (2) prepared SnO_2.

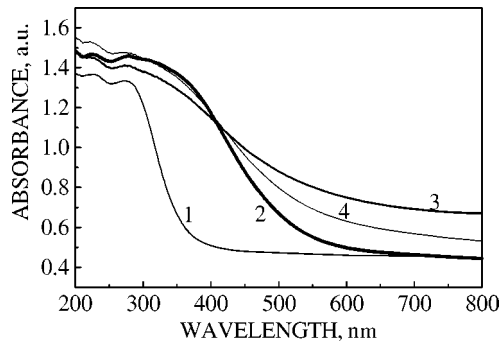

Figure 4. UV-visible DR spectra of SnO_2 after (1) outgassing at room temperature, (2) outgassing at 400 °C, (3) adsorption of CO (under 100 Torr) at room temperature and (4) outgassing at room temperature.

The formation of oxygen vacancies and Sn^{2+} ions may be described by the following equations:

$$SnO_2 \rightarrow SnO_{2-x} + xV_O + (x/2)O_{2(g)} \quad (1)$$

$$O_o^x \rightarrow V_O^{2+} + (1/2)O_{2(g)} + 2e^- \quad (2)$$

Electrons may be trapped either by ionised oxygen vacancies or by Sn^{4+}:

$$V_O^{2+} + 2e^- \rightarrow V_O \quad (2a)$$

$$Sn^{4+} + 2e^- \rightarrow Sn^{2+} \quad (2b)$$

where V_O and V_O^{2+} are the neutral and ionised oxygen vacancies, respectively, and O_o^x is lattice oxygen, according to Kröger notation [8].

3.1.2. FTIR study of adsorbed CO

CO adsorption at room temperature on SnO_2, pretreated at 400 °C first in oxygen and then *in vacuo*, gives rise to carbonyl species CO–Sn^{4+} (2200 cm^{-1}) and CO–Sn^{2+} (2145 cm^{-1}) (figure 5). To our knowledge, this observation is reported for the first time.

3.2. Characterisation of Pd/SnO_2 catalysts

Due to the lack of contrast, TEM observations give no reliable data concerning the metal particle size; however, some information is obtained from XRD line broadening.

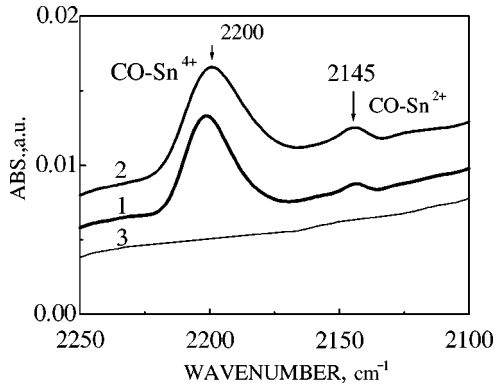

Figure 5. FTIR spectra of CO adsorbed on SnO_2 under (1) 6, (2) 30 Torr CO and (3) outgassing at room temperature.

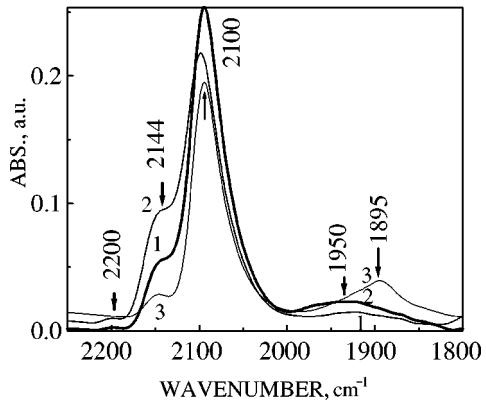

Figure 6. IR spectra of CO adsorbed on GC catalyst under (1) 5 and (2) 15 Torr CO, (3) after outgassing at room temperature.

In addition, IR spectra of adsorbed CO (figures 6, 7 and table 2) allow an estimation of the fraction of metal atoms exposed (FE) from absorbance values. Experimental conditions are chosen to avoid the drastic loss of background transmission often induced by CO adsorption (free electron absorption), that is reduction by hydrogen at temperature $\geqslant$200 °C must be avoided. Hence, CO chemisorption on the GC sample was carried out after calcination and outgassing at 400 °C.

3.2.1. GC sample

According to UV-visible DRS (not shown) [14], palladium is initially present as Pd^{2+} ions or PdO clusters (λ_{max} near 465 nm) [9], which are immediately reduced to Pd^0 upon CO chemisorption at room temperature, giving rise mainly to linear CO entities, a few bridged species and some residual ionic Pd species (figure 6). The fraction exposed estimated from absorbance value of IR bands of adsorbed CO is about 0.5 and the mean particle size deduced according to [10] is ca. 2 nm.

3.2.2. PH sample (figure 7)

The mean particle size determined from XRD is around 4.5 nm and the FE is about 0.25. Before the catalytic test, XPS shows the presence of metallic palladium (Pd $3d_{5/2}$ peak at 335.3 eV) and also of residual Pd^{2+} (Pd $3d_{5/2}$ peak

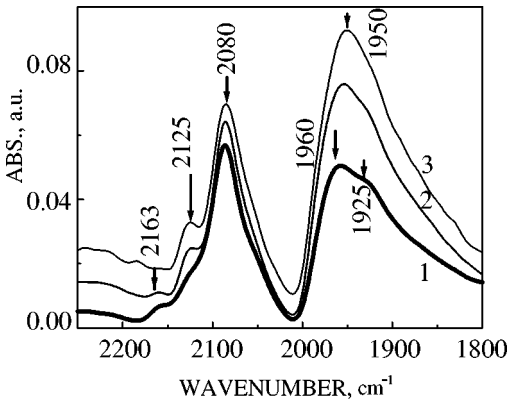

Figure 7. IR spectra of CO adsorbed on PH catalyst under (1) 5, (2) 15 and (3) 35 Torr CO.

Table 2
IR bands of CO adsorbed on SnO_2 and Pd/SnO_2.

ν (cm^{-1})	Species	References
2200	O≡C–Sn^{4+}	This work
2160–2145	O≡C–Pd^{2+}, O≡C–Sn^{2+}	[9,11,12], this work
2135–2110	O≡C–Pd^{+}	[9,11,12]
2100–2025	O≡C–Pd^0	[9–13]
1995–1960	Pd_2(CO) compressed or bridged on (100) faces	[9–12] [13]
1950–1925	Pd_2(CO) isolated or bridged on (111) faces	[9–12] [13]

at 337 eV), showing that the photoreduction process was incomplete [14].

The band positions and assignments of the CO species adsorbed on both samples and on SnO_2 are reported in table 2.

4. Catalytic performances in deNOx reaction

4.1. Reaction conditions

The reaction conditions are the following: CO (1.50 vol%), NO (0.2 vol%), O_2 (0.65 vol%) (stoichiometric gas mixture), He; space velocity (SV) = 70,000–140,000 h^{-1}; gas flow = 12 l/h; catalyst weight = 0.125–0.250 g; contact time = 0.022–0.045 s.

4.2. Results

SnO_2 alone shows a noticeable activity at 400 °C (95% CO and 65% NO conversion) (figure 8). The Pd/SnO_2 catalyst prepared by grafting and calcination (GC) is the most active with NO conversion close to 100% at temperatures as low as 180 °C, for a contact time of 0.045 s (figure 9). For the PH catalyst, NO conversion only reaches 75% at 180 °C.

4.3. Discussion

In spite of its stoichiometric nature, the gas mixture has a slight reducing effect. Before the catalytic test, the XP

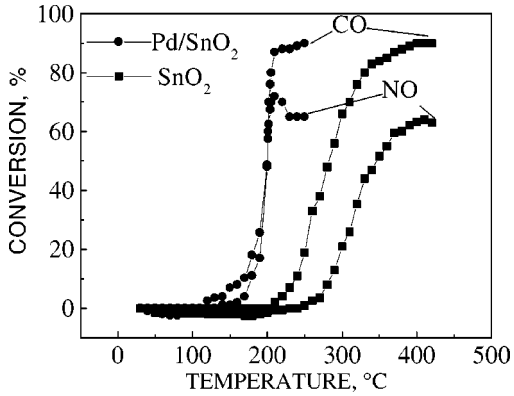

Figure 8. Catalytic activity in deNOx: SnO_2 at 400 °C, Pd/SnO_2 (GC) at 220 °C, SV = 140,000 h^{-1}.

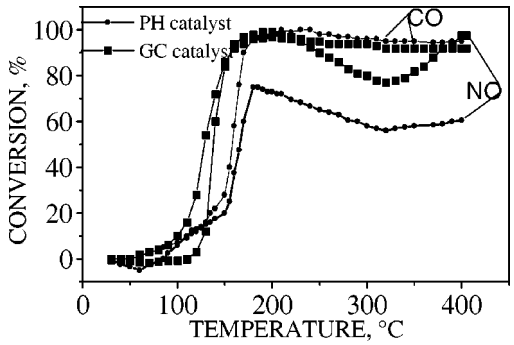

Figure 9. Catalytic activity in deNOx: (GC) and (PH) at 180 °C, SV = 75,000 h^{-1}.

spectrum of the GC sample shows only one Pd $3d_{5/2}$ peak (336.5 eV) assigned to Pd^{2+} ions. After the catalytic test, the spectrum presents two peaks at 335.5 and 337 eV; the first one is assigned to metallic palladium which demonstrates the reducing nature of this mixture, and the second one to Pd^{2+} [14].

These results show that the CO–NO–O_2 reaction takes place even on SnO_2 alone, and stresses the role of defects of this oxide (oxygen vacancies, Sn^{2+} ions). In the case of Pd/SnO_2 catalysts, it is proposed that the active sites are oxygen vacancies of the support associated with palladium atoms at the metal–support interface. The role of Pd is to adsorb CO and to enhance the formation of oxygen vacancies. The proposed mechanism involves the following steps: CO adsorbs on the metal, then spills over the support and, finally, reacts with oxygen anions of the support, generating CO_2 and oxygen vacancies according to

$$CO_{(ads)} + O_o^x \rightarrow CO_{2(g)} + V_O \quad (3)$$

These oxygen vacancies can either dissociatively trap gaseous oxygen or dissociate NO:

$$NO + V_O \rightarrow N_{(ads)} + O_o^x \quad (4)$$

$$N_{(ads)} + N_{(ads)} \rightarrow N_{2(g)} \quad (5)$$

These promising results, which stress the role of SnO_2 defects, are now being completed by electrical conductivity measurements, EPR experiments and complementary spectroscopic (UV-visible, IR) studies [14b].

Acknowledgement

The deNOx catalytic studies have been performed thanks to Professor G. Djéga-Mariadassou (Laboratoire de Réactivité de Surface, Université Pierre et Marie Curie, Paris). Engelhard-CLAL is gratefully acknowledged for palladium supply.

References

[1] (a) J.F. Aller, T. Moseley, J.O. Norris and D.E. Williams, J. Chem. Soc. Faraday Trans. I 83 (1987) 1323;
(b) G. Heiland, Sensors Actuators 2 (1982) 343.
[2] M. Sheintuch, J. Schmidt, Y. Lechtman and G. Yahav, Appl. Catal. 49 (1989) 55.
[3] J.-M. Herrmann, J. Disdier, P. Pichat, A. Fernandez, A. Gonzalez-Elipe, G. Munuera and C. Leclercq, J. Catal. 132 (1991) 490.
[4] (a) A. Trovarelli, Catal. Rev. 38 (1996) 439;
(b) S. Bernal, J.J. Calvino, M.A. Cauqui, J.M. Gatica, C. Larese, J.A. Perez Omil and J.M. Pintado, Catal. Today 50 (1999) 175;
(c) J. Kaspar, P. Fornasiero and M. Graziani, Catal. Today 50 (1999) 285.
[5] (a) M.M. Gadgil, R. Sasikala and S.K. Kulshreshtha, J. Mol. Catal. 87 (1994) 297;
(b) Y. Teraoka, T. Harada, T. Iwasaki, T. Ikeda and S. Kagawa, Chem. Lett. (1993) 773;
(c) M.J. Fuller and M.E. Warwick, Chem. Ind. (1976) 787.
[6] S.P. Tandon and J.P. Gupta, Phys. Stat. Sol. 38 (1970) 363.
[7] G. Ghiotti, A. Chiorino, G. Martinelli and M.C. Carotta, Sensors Actuators B 24/25 (1995) 520.
[8] P.A. Cox, *Transition Metal Oxides* (Clarendon Press, Oxford, 1992).
[9] D. Tessier, A. Rakaï and F. Bozon-Verduraz, J. Chem. Soc. Faraday Trans. 88 (1992) 741.
[10] J. Benson and M. Boudart, J. Catal. 4 (1964) 704.
[11] Y.A. Lokhov and A. Davydov, Kinet. Katal. 21 (1980) 1515, 1523.
[12] C. Naccache, M. Primet and M. Mathieu, Adv. Chem. Ser. 121 (1973) 266.
[13] A. Badri, C. Binet and J.C. Lavalley, J. Phys. Chem. 86 (1989) 451.
[14] (a) D. Amalric, F. Bozon-Verduraz and D. Fatu, in: *4th European Congress on Catalysis*, Rimini, 1999;
(b) D. Amalric, J.-M. Herrmann, A. Ensuque and F. Bozon-Verduraz, to be published.